J. Agr. Sci. Tech. (2013) Vol. 15: 1319-1334

Experiments on Variable-mass Threshing of Rice in the Tangential-longitudinal-flow Combine Harvester

T. Zhong[1]*, L. Yaoming[1], and W. Chenghong[1]

ABSTRACTA

The existing studies of threshing process of combine harvesters adopt the assumption of constant mass, which is contradictory to the phenomenon of separation of grains and short stalks in actual threshing process. Therefore, the characteristics of threshing and separation are not accurately described. Aiming at this problem, this study established the tangential-longitudinal threshing and separation test-bed with tangential-flow device, auxiliary feed beater, and longitudinal-flow device of tangential-longitudinal-flow combine harvester and conducted experiments and analysis of rice threshing with feed rates of 5, 6, and 7 kg s^{-1}. The results showed that the changes in rates of material flow along the arc-length of concave in tangential-flow device and longitudinal-flow device were equal to the changes in rates of material density with time. In the process of variable-mass and constant-mass rice threshing, when the feeding rates were 5, 6, and 7 kg s^{-1} in the test-bed, the flow rates from the tangential-flow device were 4.07, 5.01, and 5.95 kg s^{-1}, respectively. The average power consumption of the tangential-flow drum in variable mass threshing process was higher than that in the constant mass threshing process by 2.16, 2.73, and 3.09kW, respectively. The flow rate at the outlet of the longitudinal-flow device was 3.34, 4.04, and 4.72 kg s^{-1}, respectively. The average power consumption rate of the longitudinal-flow drum in variable mass threshing process was lower than that in the constant mass threshing process by 7.32, 10.44, and 12.17kW, respectively. The results of material flow rate and power consumption would offer the basis for the design of longitudinal-tangential flow threshing and separation device.

Keywords: Harvesting rice, Material flow rate, Power consumption, Tangential-longitudinal threshing drum, Threshing and separation process, Tooth structure.

INTRODUCTION

The threshing and separation unit is the core device of combine harvester, which also determines the working performance of the whole machine (Saeid *et al.*, 2006; Su, *et al.*, 2012). Studying material threshing performance in the combine harvester is the key to improvement of harvesting performance (Wacker and Kutzbach, 2003; Rahimi, *et al.*, 2010). Previous studies assumed that the material mass remained the same from the entrance to the outlet of the threshing space, for example, when studying the working process of the threshing and separation device of combine harvester. Scientists of Chinese Academy of Agricultural Mechanization Sciences, adopted constant mass threshing and separation theory to establish equation of threshing rate and separation rate of the threshing and separation device (Yang and Yan , 2008; Li *et al.*, 2006). Huynh and Powell (1982) and Anil *et al.* (1998) believed that the velocity of straw in the threshing space was equal to the circumferential velocity of the drum and adopted constant mass threshing and separation theory to develop threshing rate

[1] Key Laboratory of Modern Agricultural Equipment and Technology, Ministry of Education and Jiangsu Province, Jiangsu University, Zhenjiang, Jiangsu, China.
*Corresponding author; e-mail: tangzhong2012@gmail.com

[DOR: 20.1001.1.16807073.2013.15.7.20.9]

and separation rate model. However, during the threshing process, grains and short stalks of most threshing material were separated through the concave, with great effect on the characteristics of dynamics and kinematics of the system. If the mass change is ignored when we study the threshing and separation performance, the result of the study would be quite different.

To analyze the effect of the variable mass on the threshing and separation performance, Zhang and Sang (2000), from the University of Science and Technology of China, conducted the non-linear mathematical model of the material movement during tangential-flow threshing process as well as set thorough power consumption model of tangential-flow threshing drum based on the fundamentals of variable mass system. Scholars from the Hohenheim University in Germany established the longitudinal-flow threshing equation by modeling and analyzing the longitudinal-flow drum based on the variable mass theory during the threshing process (Miu and Kutzbach, 2007; Miu, 2008). Most scientists have developed the tangential-flow threshing model or longitudinal-flow threshing model according to the variable mass theory (Kumara *et al.*, 2002; Sudajana *et al.*, 2002; Mostofi and Minaei, 2009), while few have analyzed the rate of flow of the material in the threshing and separation device and the effect of the variable mass on the power consumption during the threshing process (Szymanek, 2008; Godwin *et al.*, 1999; Hennens *et al.*, 2003; Maertens and Baerdemaeker, 2003).

In order to discuss the assumption of constant mass which is contradictory to the phenomenon of separation of grains and short stalks in actual threshing process, tangential-longitudinal threshing and separation test-bed was established to conduct experiments and analyze rice threshed with feed rates of, 5, 6 and 7 kg s^{-1}. The change in rates of the material flow of tangential-flow device and longitudinal-flow device was studied to obtain the normal operation requirement. The relationship between experimental and theoretical material flow rate was studied to obtain the characteristic of threshing and separation. The average power consumptions of the tangential-flow drum, auxiliary feed beater, and longitudinal-flow drum during the threshing process in the variable mass and constant mass were recorded, respectively, through the torque sensor to measure the threshing torque and the speed of tangential-longitudinal threshing drum.

MATERIALS AND METHODS

This study was divided into three main sections:

1) Material flow studies in the threshing and separation unit of tangential-longitudinal- flow combine harvester.

2) Variable mass test of material flow rate of the tangential-longitudinal threshing and separation test-bed during the threshing process.

3) Comparison of power consumption to evaluate the difference of the variable mass and constant mass during the threshing process.

Test of Rice Material and Torque Sensors

The rice tested was WU‘2645’ (a type of rice that grows in Jiangsu province of China), with the average height of 1,050 mm and the average spike length of 166 mm. The average one-thousand kernel weight was 28.5 g and the average grain output was 10,275 kg ha^{-1}. Average grain to MOG (material other than grain) ratio was 2.86:1 and the average moisture content of the stalks and the kernels was, respectively, 66.43 and 25.02%.

The tangential-flow drum, auxiliary feed beater, and the longitudinal-flow drum were driven by the frequency conversion motors and, during the threshing process, three HAD-CYB-803S torque sensors (produced by Beijing Heng Odd Instrument Co., Ltd.)

[DOR: 20.1001.1.16807073.2013.15.7.20.9]

were used to measure the torque value and speed (the measurement accuracy was 0.25% FS and the frequency response time was 100 μs).

Threshing and Separation Test-bed

Tangential-longitudinal-flow combine harvester consisted of cutter, inclined conveyor, tangential-flow drum, auxiliary feed beater, longitudinal-flow drum, fans, vibrating sieve, handle system, chassis, etc. A test-bed of the key part of the threshing and separation unit of the longitudinal-tangential-flow combine harvester was set in the laboratory in order to analyze the effect that the variable mass had on the performance of threshing and separation process. The test-bed was made of tangential-flow drum, auxiliary feed beater, longitudinal-flow drum, torque sensors, motors, transmission system, and tilted conveyor, etc. The main structure of the test-bed is shown in Figure 1.The reception boxes were fixed under the grid concave of the longitudinal-flow drum and tangential-flow drum to receive the grains and short stalks separated through the grid concave, of which 13 reception boxes were fixed along the axial direction of the longitudinal-flow drum.

The diameter of the tangential-flow drum was 490 mm and the length was 1,125 mm. The arrangement of knife tooth threshing components was four head spiral with the 55 mm insert spacing. The height of the knife tooth was 70 mm with a thickness of 4 mm. There were knife tooth in the corresponding concave grid with concave wrap of 80° (Igathinathane *et al.*, 2008; Tang *et al.*, 2011), and the concave clearance at the entrance and output was, respectively, 40 and 30 mm. The speed of the tangential-flow drum was 10.26 m s^{-1} (Vejasit and Salokhe, 2005). The assembled relation of the concave and the tangential-flow drum and structure of knife tooth are shown in Figure 2.

The diameter of the longitudinal-flow drum was 500 mm, with the total length of 3350 mm. There were helical blades with a length of 170 mm in front of the longitudinal-flow drum, trapezoidal tooth within the central 2,700 mm and the discharge plate at the rear of the longitudinal-flow drum. Cylinder concave clearance was 30 mm and the angle of the wrap of concave was 180°. Four lines threshing components were mounted at equal distance of 150 mm along axial direction on the circumference of longitudinal-flow drum. The longitudinal-flow drum speed was 11.12 m s^{-1} (Harrison, 1991; Rasouli, *et al.*, 2009). Side view of the longitudinal-flow drum and trapezoidal tooth are shown in Figure 3.

Rice Threshing Process and Flow Direction

During the threshing process, the rice with constant mass just cut from the field was

(a) Photo of the threshing device.

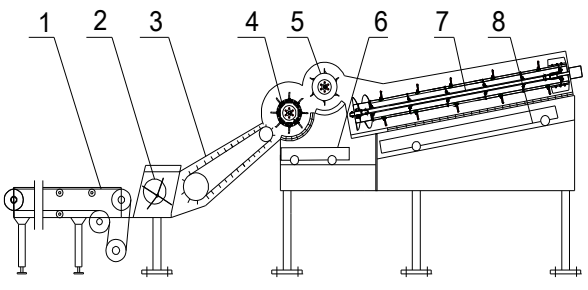

(b) Schematic diagram of structure.

Figure 1. Schematic diagram of tangential-longitudinal threshing and separation test-bed: (1) Conveyer belt; (2) Feeding auger; (3) Spout; (4) Tangential-flow drum; (5) Auxiliary feed beater; (6) Tangential-flow reception box; (7) Longitudinal-flow drum, (8) longitudinal-flow reception box.

[DOR: 20.1001.1.16807073.2013.15.7.20.9]

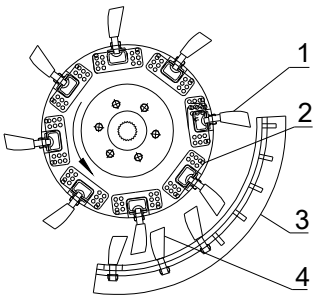

(a) Structure of tangential-flow drum and concave grid.

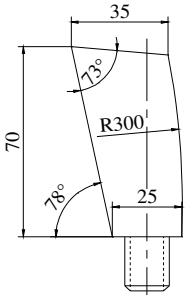

(b) Knife tooth structure.

Figure 2. Structure diagram of tangential-flow drum and concave grid with knife tooth: (1) Knife tooth threshing component; (2) Tangential-flow drum; (3) Concave grid, (4) Knife tooth of the concave grid.

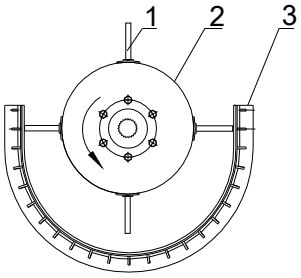

(a) The structure of longitudinal-flow drum and concave grid.

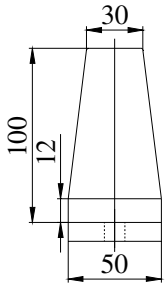

(b) The structure of trapezoidal tooth threshing component.

Figure 3. Diagram of longitudinal-flow drum and trapezoidal tooth: (1) Trapezoidal tooth threshing component; (2) Longitudinal-flow drum, (3) Grid concave.

evenly put on the conveyor belt at the liner speed of 1 m s^{-1}. The rice was transported to the feeding auger by the conveyer belt and, then, the feeding auger put the rice into the spout. The rice went to the tangential-flow drum from the spout, then, the rice was primarily threshed by the threshing component of the tangential-flow drum. After that, under the action of auxiliary feeding beater the rice fell to the longitudinal-flow drum and was further threshed. At last, the straw was let out from the grass discharge at the rear part. The mixtures ran into the tangential-flow reception boxes or longitudinal-flow reception boxes through concave grid. Then, the performance index (power consumption, grain flow rate, stalk flow rate, and grain or stalk flow rate proportion) of threshing of the tangential-flow drum and the longitudinal-flow drum was determined manually.

The flow direction and path of the rice in the tangential-longitudinal flow device are shown in Figure 4.

The direction of arrow shows the material flow direction, while the "*a~a*" and "*b~b*" cross sections depict, respectively, the input and output part of the tangential-flow device. The "*c~c*" and "*d~d*" cross sections show the input and output part of the auxiliary feed device, respectively. The "*e~e*" and "*f~f*" cross sections represent the input and output part of the longitudinal-flow device, respectively.

Different symbols are used to show the mass flow process through this device. Thus,

dt= Time interval that the material flows from "*a~a*" cross section to "*b~b*",

q_a= The feed rate of the material at the "*a~a*" cross section with the flow density of k_a,

q_a–dq_a= The feed rate at the "*b~b*" cross section , where dq_a stands for the variation of the material flow,

[DOR: 20.1001.1.16807073.2013.15.7.20.9]

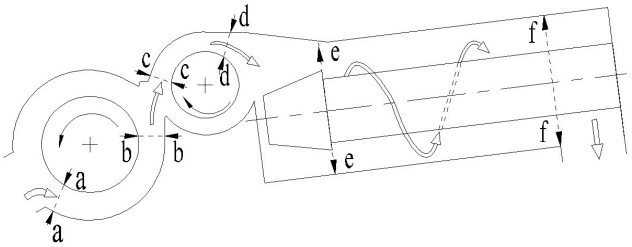

Figure 4. The rice flow direction in the tangential-longitudinal flow device.

k_a–dk_a= Flow density, where, dk_a stands for the variation of density,

ds_a= Arc length of the concave grid,

$v_{b=}$ Average speed of the material at the output part of the tangential-flow device, with a density of k_b and a feeding rate of q_b; because the feeder beater did not have the function of threshing but acted as feeder,

v_c= The speed of the material at "*c*~*c*", with a density of k_c and a material flow rate of q_c,

v_d= Average speed of the material at "*d*~*d*", with a density of k_d and a material flow rate of q_d, all the parameters of which were the same as "*c*~*c*" cross section.

Thus, the section from the "*c*~*c*" to "*d*~*d*" cross section is considered as the transitional part and the speed of the material at the "*c*~*c*" and "*d*~*d*" cross sections is denoted as v_{cd}, with density of k_{cd} and material flow rate of $q_{cd.}$

dt_e= The time interval for material flow from the "*e*~*e*" to "*f*~*f*" cross section , with the feeding rate at the "*e*~*e*" cross section as q_e and density of k_e. The feeding rate at the "*f*~*f*" cross section is shown by q_f –dq, in which dq stands the change in quantity of the material flow rate, with density of k_e–dk_e, where, dk_e stands for the change in the density, and ds_e represents the length of the concave grid of the longitudinal-flow drum.

Variable Mass Power Consumption

Burcev (1963), from the Institute for Theoretical Physics at the J. E. Purkyně University, deduced the motion equation of the variable mass of Meshchersky equation. Meshchersky's equations was used to describe the variable mass in the threshing process, with the variable mass equation during the longitudinal-flow threshing process as follows:

$$m\frac{dv}{dt}-\frac{dm}{dt}(u_0-v_0)=F \quad (1)$$

Where, m is the mass of the longitudinal-flow drum plus the feed material, dm is the mass of the grains separated, v_0 the absolute speed of the longitudinal- flow drum, u_0 the absolute speed of the grains separated, F as the resultant force that the longitudinal-flow drum was subjected to, and dm/dt was the change in the rate of the grain mass with time. Because the grains were being separated into the boxes, the value of the dm/dt was below zero.

The grains were separated continuously during the threshing process, then, the speed gap between the grain speed and the stalk speed was v_r. That is v_r= u_0–v_0. Thus,

$$\frac{dm}{dt}v_r=F_r \quad (2)$$

Where, F_r represents the force that grains exert on the longitudinal-flow drum. From the Equation (1) and (2) we could get

$$m\frac{dv}{dt}=F+F_r \quad (3)$$

Thus, the torque value of the longitudinal-flow drum T is:

$$T=(F+F_r)R \quad (4)$$

In which, R is the torture length of longitudinal-flow drum and, according to the Equation (4) we could get the longitudinal-flow drum power consumption P:

$$P=\frac{Tn}{9550} \quad (5)$$

[DOR: 20.1001.1.16807073.2013.15.7.20.9]

Where, n is the speed of the longitudinal-flow drum during the threshing process.

RESULTS AND DISCUSSION

Variable Material Flow in Threshing and Separation Unit

According to the law of conservation of mass, difference of the feeding mass at the "*a~a*" and at the "*b~b*" cross sections equals the mass of the grains separated from the tangential-flow device, therefore:

$$[q_a-(q_a-dq_a)]dt_a=[k_a-(k_a-dk_a)]ds_a \quad (6)$$

From Equation (6), we could derive the following:

$dq_a dt_a = dk_a ds_a$, which can be changed to Equation (7)

$$\frac{dq_a}{ds_a}=\frac{dk_a}{dt_a} \quad (7)$$

From Equation (7), the change in rate of the material mobility, q_a, along the arc length s_a equals the change in the rate of the density, k_a, with the time t_a.

When the material gets into the longitudinal-flow device from the auxiliary feeding device, the flow mass of material in the time t_c is Q_{cd}, and

$$Q_{cd}=(v_b-v_{cd})k_b t_c=(v_e-v_{cd})k_e t_c \quad (8)$$

And the Equation (9) could be deduced as follow:

$$(v_b-v_{cd})k_b=(v_e-v_{cd})k_e \quad (9)$$

We could derive the following:

$$v_{cd}=\frac{v_b k_b-v_e k_e}{k_b-k_e} \quad (10)$$

Since the material flow rate at the "*b~b*" cross section of the tangential-flow device is q_b, and the material flow rate at the "*e~e*" cross section of the longitudinal-flow device is q_e, we could write the following by the definition:

$$\begin{cases} q_b=k_b v_b \\ q_e=k_e v_e \end{cases} \quad (11)$$

By putting these parameters in Equation (10), we could get Equation (12):

$$v_{cd}=\frac{q_b-q_e}{k_b-k_e} \quad (12)$$

Because the material quantity $q_b t_c$ at the "*b~b*" cross section of the tangential-flow device in unit time equals the material quantity $q_{cd}t_c$ of the feeding device and it is also equal to the feeding quantity $q_e t_c$ at the "*e~e*" cross section, i.e. $q_b t_c = q_{cd}t_c = q_e t_c$, then, when $q_b > q_e$ and $k_e < k_b$, v_{cd} becomes negative, which means that the feeding device would be blocked up. On the other hand, when $q_b < q_e$ and $k_e > k_b$, v_{cd} is positive, which means that the feeding device is in good operation.

According to the law of conservation of mass, the difference between feeding quantity at the "*e~e*" and at the "*f~f*" cross sections are equal to the quantity of the grains of the concave grid, then:

$$[q_e-(q_e-dq_e)]dt_e=[k_e-(k_e-dk_e)]ds_e \quad (13)$$

From which, we could obtain $dq_e dt_e = dk_e ds_e$, and Equation (14):

$$\frac{dq_e}{ds_e}=\frac{dk_e}{dt_e} \quad (14)$$

According to the Equation (14), the change in material flow rate, q_e, with the axial length of the concave grid s_e equals the change of the material density k_e within the time interval t_e.

Therefore, the change in the rate of the material flow rate q_a of the tangential-flow device along the arc length s_a of the grid concave equals the change in the rate of the material density k_a in the time interval t_a; when $q_b > q_e$ and $k_e < k_b$, v_{cd} is negative, which means that the feeding device would be blocked up; when $q_b < q_e$ and $k_e > k_b$, v_{cd} is positive, which indicates that the feeding device is in good operation. The change in the rate of the material flow rate q_e along the axial length s_e of the grid concave equals the change in the rate of the material flow density k_e in the time interval t_e.

[DOR: 20.1001.1.16807073.2013.15.7.20.9]

Variable Mass Test of Material Flow Rate

The tested rice of 60, 72, and 84 kg just cut from the field were put on the conveyer belt with the type of 12000×1000 mm and the liner speed of the conveyer was 1 m s^{-1}(feeding rate was 5, 6, and 7 kg s^{-1}), and the feeding time was 12 seconds. The grains and the mixtures were weighed manually (the electronic scale was JY60001, Shanghai Fangrui Instrument Co., Ltd., the measurement accuracy of the electronic scale was 0.1 g, and the maximum range was 6 kg) and the results are shown in Table 1.

Since the material was fed continuously and with even flow rate feeding within 12 seconds, we could calculate the grain mass and the mixture mass per second (flow rate of grains and flow rate of mixtures). The values of the material experimental flow rate, grains flow rate, and stalk flow rate of each box were calculated and are shown in Table 2.

Based on the results in Table 2, Figure 5 shows the percentage that the experimental material flow rate accounted for the theoretical feeding rates of 5, 6 and 7 kg s^{-1}, respectively. The tangential-flow device corresponded to the point 0 of coordinate axis and the longitudinal-flow device corresponded to the points 1 to 13.

From Figure 5, we could see that when the feeding rate was 5, 6, and 7 kg s^{-1}, the percentage was, respectively, 81.470, 83.536, and 85.001% at the tangential-flow device, and the percentage of the first reception box of the longitudinal-flow device was, respectively, 80.006, 81.699, and 83.073%, while the corresponding percentages of the thirteenth reception box were only 67.324, 67.339, and 67.442%. Thus, we could know that the experimental material flow rate was less than the theoretical feed rate within the tangential-flow device and the longitudinal-flow device.

Table 1. The weight of the material in the reception boxes (kg).

Test item	Tangential reception box	Reception box number along axial direction of longitudinal-flow drum under grid concave												
		1	2	3	4	5	6	7	8	9	10	11	12	13
Grains weight at 5 kg s^{-1}	9.152	0.677	1.779	1.371	0.691	0.501	0.444	0.222	0.197	0.146	0.094	0.074	0.047	0.100
Mixture weight at 5 kg s^{-1}	1.965	0.201	0.321	0.249	0.211	0.213	0.162	0.131	0.152	0.122	0.105	0.093	0.097	0.087
Grains weight at 6 kg s^{-1}	9.690	1.070	2.284	1.793	0.959	0.908	0.544	0.385	0.291	0.190	0.140	0.097	0.060	0.038
Mixture weight at 6 kg s^{-1}	2.164	0.253	0.361	0.355	0.290	0.316	0.274	0.188	0.184	0.166	0.153	0.135	0.130	0.100
Grains weight at 7 kg s^{-1}	10.259	1.323	2.849	2.438	1.279	1.227	0.674	0.459	0.349	0.253	0.197	0.138	0.092	0.079
Mixture weight at 7 kg s^{-1}	2.340	0.296	0.422	0.414	0.339	0.369	0.320	0.220	0.215	0.193	0.178	0.157	0.152	0.117

[DOR: 20.1001.1.16807073.2013.15.7.20.9]

Table 2. Feeding rate and experimental flow rate of each pair of boxes within tangential-longitudinal device.

Test item	Tangential-reception box	Reception box number along axial direction of longitudinal-flow drum under grid concave												
		1	2	3	4	5	6	7	8	9	10	11	12	13
Feeding rate at 5 kg s^{-1}	5	5	5	5	5	5	5	5	5	5	5	5	5	5
Experimental flow rate (kg s^{-1})	4.074	4.000	3.825	3.690	3.615	3.556	3.505	3.476	3.447	3.424	3.408	3.394	3.382	3.366
Grain flow rate (kg s^{-1})	0.533	0.477	0.328	0.214	0.157	0.115	0.078	0.059	0.043	0.031	0.023	0.017	0.013	0.004
Stalk flow rate (kg s^{-1})	3.540	3.524	3.497	3.476	3.459	3.441	3.427	3.416	3.404	3.394	3.385	3.377	3.369	3.362
Flow rate proportion (%)	81.470	80.006	76.507	73.808	72.303	71.113	70.103	69.514	68.932	68.484	68.154	67.876	67.635	67.324
Feeding rate at 6 kg s^{-1}	6	6	6	6	6	6	6	6	6	6	6	6	6	6
Experimental flow rate (kg s^{-1})	5.012	4.902	4.682	4.503	4.399	4.297	4.228	4.181	4.141	4.111	4.087	4.068	4.052	4.04
Grain flow rate (kg s^{-1})	0.738	0.649	0.459	0.309	0.230	0.154	0.109	0.077	0.052	0.036	0.025	0.017	0.012	0.008
Stalk flow rate (kg s^{-1})	4.274	4.253	4.223	4.193	4.169	4.143	4.120	4.104	4.089	4.075	4.062	4.051	4.040	4.032
Flow rate proportion (%)	83.536	81.699	78.026	75.043	73.309	71.609	70.473	69.677	69.017	68.523	68.117	67.795	67.53	67.339
Feeding rate at 7 kg s^{-1}	7	7	7	7	7	7	7	7	7	7	7	7	7	7
Experimental flow rate (kg s^{-1})	5.950	5.815	5.543	5.305	5.170	5.037	4.954	4.898	4.851	4.813	4.782	4.758	4.737	4.721
Grain flow rate (kg s^{-1})	0.961	0.851	0.613	0.410	0.303	0.201	0.145	0.107	0.078	0.057	0.040	0.029	0.021	0.014
Stalk flow rate (kg s^{-1})	4.989	4.965	4.929	4.895	4.867	4.836	4.809	4.791	4.773	4.757	4.742	4.729	4.716	4.706
Flow rate proportion (%)	85.001	83.073	79.180	75.784	73.858	71.958	70.775	69.966	69.295	68.763	68.317	67.966	67.675	67.442

[DOR: 20.1001.1.16807073.2013.15.7.20.9]

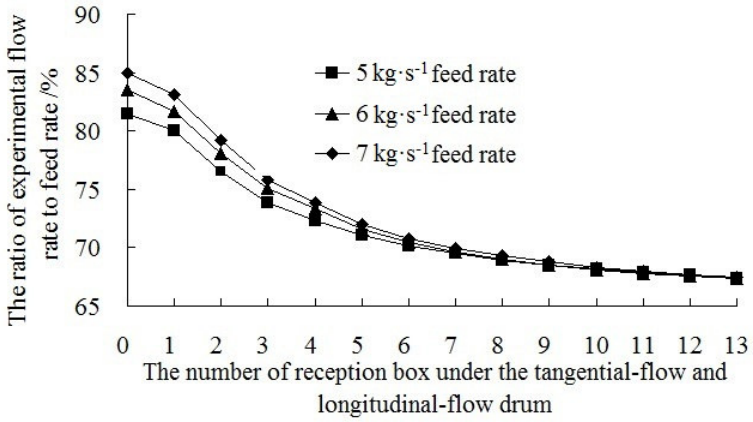

Figure 5. The percentage that the experimental material flow rate accounted for the theoretical feeding rates at the speed of 5, 6, and 7 kg s^{-1}.

based on the results shown in Table 2, we used data fitting software DPS(Data Processing System) to determine regression correlation between the experimental material flow rate q_a and the feed rate q_{a0} at the feed rate of 5 kg s^{-1}, and the result is shown below in Equation (15), with the correlation coefficient of 0.9983.

$$q_a = [67.263 + 17.0223e^{-0.301942n}]q_{a0} \quad (15)$$

Similarly, we got the percentage relations between the experimental material flow rate q_b and the feed rate q_{b0} for the feed rate of 6 kg s^{-1} and the result is shown below in Equation (16), with the correlation coefficient of 0.9996.

$$q_b = [66.9507 + 19.5478e^{-0.285101n}]q_{b0} \quad (16)$$

The percentage relations between the experimental material flow rate q_c and the feed rate q_{c0} at the feed rate of 7 kg s^{-1} and the result was shown as below in Equation (17) and the related coefficient was 0.9994.

$$q_c = [67.0964 + 21.3847e^{-0.291322n}]q_{c0} \quad (17)$$

Thus, the experimental flow rate was less than the theoretical feed rate in the tangential-flow device and longitudinal-flow device at the feed rate of 5, 6, and 7 kg s^{-1}. The experimental flow rate had a nearly exponential relationship with the feed rate in the longitudinal-flow device.

In order to analyze the grain flow rate during the threshing process in tangential-flow device and longitudinal-flow device, based on Table 2, the relation between the grain experimental flow rate and stalk flow rate at the speed of 5, 6, and 7 kg s^{-1} are depicted in Figures 6-8.

According to Figure 6, when the feed rate was 5 kg s^{-1}, the experimental material flow rate of the tangential-flow device was 4.074 kg s^{-1}, the grains flow rate was 0.533 kg s^{-1}, and the stalk flow rate was 3.540 kg s^{-1}, while the grains threshed and separated by the tangential-flow device accounted for 58.862% of total grains. The grain flow rate decreased from 0.477 kg s^{-1} at the position of reception box 1 (RB1) to 0.043 kg s^{-1} at the position of the RB8, with the change of grain flow rate of 0.434 kg s^{-1}. The grain flow rate decreased from 0.031 kg s^{-1} at the position of RB10 to 0.004 kg s^{-1} at the position of RB13, at the rate of 0.027 kg s^{-1}. Thus, about 37.834% of grains were separated from the first to the eighth RB, and 2.961% of grains were separated from the ninth to the thirteenth RB and the grain loss proportion was 0.343%. The stalk flow rate changed from 3.524 kg s^{-1} at the position of RB1 to 3.394 kg s^{-1} at the position of RB 9, at a rate of 0.13 kg s^{-1}. The stalk flow rate changed from 3.385 kg s^{-1} at the position of

[DOR: 20.1001.1.16807073.2013.15.7.20.9]

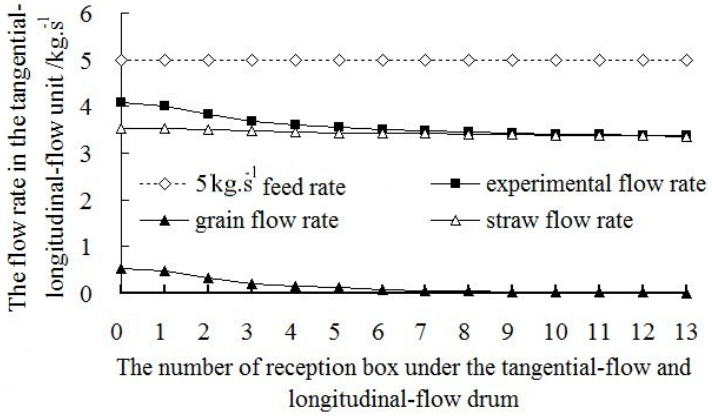

Figure 6. The experimental grains and stalk flow rate at the feed rate of 5 kg s^{-1}.

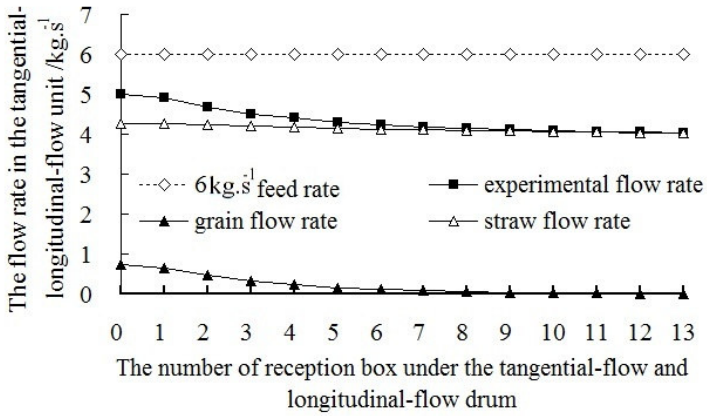

Figure 7. The experimental flow rate of the grains and the stalk at the feed rate of 6 kg s^{-1}.

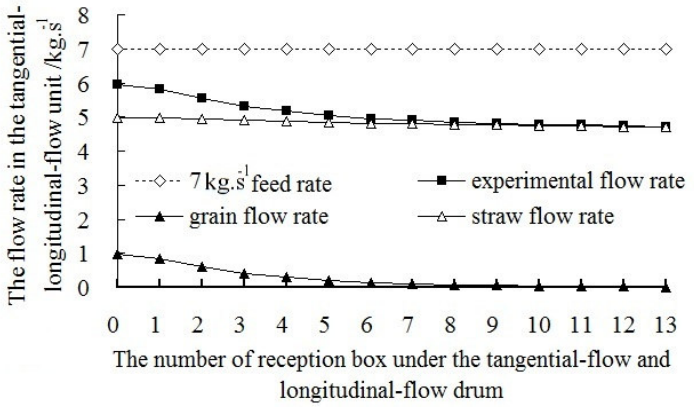

Figure 8. The experimental flow rate of the grains and the stalk at the feed rate of 7 kg s^{-1}.

RB10 to 3.362 kg s^{-1} at the position of RB13, at the rate of 0.023 kg s^{-1}. Thus, about 3.965% of stalk mixture was separated from the first to the ninth RB while 0.861% stalk was separated from the tenth to the thirteenth RB.

According to Figure 7, the experimental material flow rate was 5.012 kg s^{-1} at the feed rate of 6 kg s^{-1}, the grain flow rate was 0.738 kg s^{-1} and the stalk flow rate was 4.274 kg s^{-1}, and grains threshed and separated by the tangential-flow device accounted for 52.242 % of total grains. The

[DOR: 20.1001.1.16807073.2013.15.7.20.9]

grain flow rate changed from 0.649 kg s^{-1} at the position of RB1 to 0.052 kg s^{-1} at the position of RB8, at a rate of 0.597 kg s^{-1}. The grain flow rate decreased from 0.036 kg s^{-1} at the position of RB10 to 0.008 kg s^{-1} at the position of RB13, at a rate of 0.028 kg s^{-1}. Thus, we could see that about 44.377% of grains were separated from the first to the eighth RB while 2.833% stalk was separated from the ninth to the thirteenth RB and the grain loss proportion was 0.548%. The stalk flow rate changed from 4.253 kg s^{-1} at the position of RB1 to 4.075 kg s^{-1} at the position of RB 9 with a change of 0.178 kg s^{-1}, and the stalk flow rate decreased from 4.062 kg s^{-1} at the position of RB10 to 4.032 kg s^{-1} at the position of RB13 at a rate of 0.03 kg s^{-1}. Thus, about 4.467% of stalk mixture was separated from the first to the ninth RB and 0.968% of the stalk was separated from the tenth to thirteenth RB.

According to Figure 8, the material flow rate was 5.950 kg s^{-1} while the flow rate of grain and the stalk was, respectively, 0.961 and 4.989 kg s^{-1} at the feed rate of 7 kg s^{-1}. Grains threshed and separated by the tangential-flow device accounted for 47.082% of total grains. The grain flow rate changed from 0.851 kg s^{-1} at the position of RB1 to 0.078 kg s^{-1} at the position of RB 8, at the rate of 0.773 kg s^{-1}. The grain flow rate decreased from 0.057 kg s^{-1} at the position of RB10 to 0.014 kg s^{-1} at the position of RB13 at the rate of 0.043 kg s^{-1}. To sum up, about 48.638% of grains were separated from the first to the eighth RB while 3.484% of stalk was separated from the ninth to the thirteenth RB and the grain loss proportion was 0.794%. The stalk flow rate changed from 4.965 kg s^{-1} at the position of RB 1 to 4.757 kg s^{-1} at the position of RB 9 with a change of 0.208 kg s^{-1}. The stalk flow rate decreased from 4.742 kg s^{-1} at the position of RB10 to 4.706 kg s^{-1} at the position of RB 13 at a rate of 0.036 kg s^{-1}, from which we could see that 4.482% of the stalk mixture was separated from the first to the ninth RB and about 0.971% of stalk were separated from the tenth to thirteenth RB.

Power Consumption of Variable Mass and Constant Mass

The test was conducted at the feed rate of 7 kg s^{-1}, and the power consumption of the tangential-flow drum, auxiliary feed beater, and the longitudinal-flow drum were obtained during the threshing process under the variable mass and constant mass conditions. HAD-CYB-803S torque sensor was used to measure torque value and speed of tangential-flow drum, auxiliary feed beater, and longitudinal-flow drum under variable and constant mass during the threshing process. The power consumption was calculated based on the measured torque value and speed. Curves of power consumption versus time of the tangential-flow drum, auxiliary feed beater and the longitudinal-flow drum are shown in Figures 9-11.

According to Figure 9, when the tangential-flow drum was in the constant mass threshing process, the curve fluctuated and the maximum value was 17.34kW and the average power consumption was 9.75kW, the instantaneous power consumption was unstable and the curve was irregular. When the tangential-flow drum was in the variable mass threshing process, the curve fluctuated and had a maximum value of 23.33kW with the average power consumption of 12.84kW. The instantaneous power consumption was unstable and the curve was irregular. We could see that the maximum and the average power consumptions in the variable mass were, respectively, 5.99 and 3.09kW more than that in the constant mass case.

According to Figure 10, when the auxiliary feed device was in variable mass threshing process, the maximum value was 15.82kW and the average power consumption was 6.78kW. When the auxiliary feed device was in constant mass threshing process, the maximum value was 16.31kW and the average power consumption was 8.43kW. Thus, the maximum and the average power consumptions of auxiliary feed device in variable mass were, respectively, 0.49

[DOR: 20.1001.1.16807073.2013.15.7.20.9]

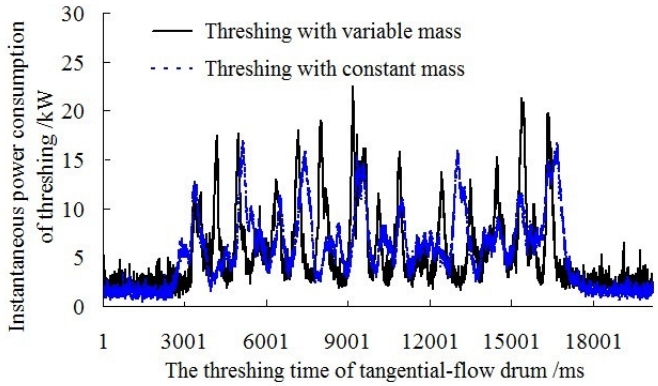

Figure 9. The power consumption curve of the tangential-flow drum at the feed rate of 7 kg s^{-1} under variable and constant mass conditions.

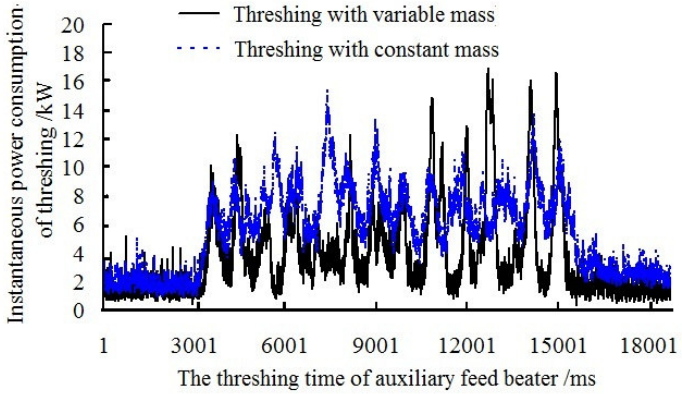

Figure 10. The power consumption curve at the feed rate of 7 kg s^{-1} at the auxiliary feed beater under variable and constant mass conditions.

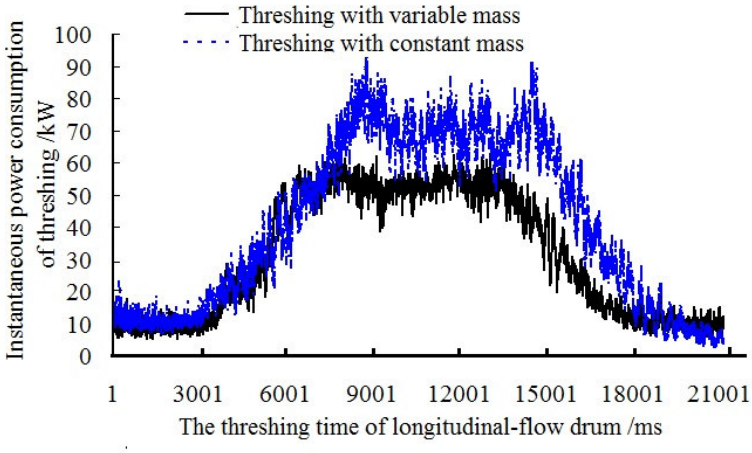

Figure 11. The power consumption curve of the longitudinal-flow drum at the feed rate of 7 kg s^{-1} under variable and constant mass conditions.

[DOR: 20.1001.1.16807073.2013.15.7.20.9]

and 1.65kW less than that in the case of constant mass.

According to Figure11, when the longitudinal-flow drum was in variable and constant mass during the threshing process, the power consumption curve had a trapezoidal shaped. The average and the maximum power consumptions in variable mass were, respectively, 52.77kW and 66.17kW, while the average and the maximum power consumptions in constant mass were, respectively, 64.94 and 87.24kW. Thus, the average and the maximum power consumptions in variable mass were, respectively, 12.17 and 21.07kW less than that in the constant mass case.

The maximum and the average power consumption of the longitudinal-flow drum, the tangential-flow drum, and the auxiliary feed device at the feed rate of 7 kg s^{-1} are shown in Table 3.

Similarly, the maximum and the average power consumption of the longitudinal-flow drum, the tangential-flow drum, and the auxiliary feed beater in variable mass and constant mass at the feed rate of 5 and 6 kg s^{-1} are shown in Tables 4 and 5.

According to Table 4, when the longitudinal-tangential-flow device was at the feed rate of 6 kg s^{-1} in variable and constant mass, the average power consumption of the tangential-flow drum in variable mass was 2.73kW more than that in the constant mass and the maximum power consumption difference was 4.28kW. The average and the maximum power consumptions of the auxiliary feed beater in variable mass were, respectively, 1.24 and 0.37kW less than that in the case of constant mass. The average and the maximum power consumptions of the longitudinal-flow drum in variable mass were, respectively, 10.44and 18.76kW less than that in constant mass case.

According to Table 5, when the threshing device of tangential-flow drum was at the feed rate of 5 kg s^{-1} in variable and constant mass, the average power consumption of the tangential-flow drum in variable mass was 2.16kW more than that in constant mass and the maximum difference was 3.64kW. The average and the maximum power consumptions of the auxiliary feed beater in variable mass were, respectively, 0.86 and 0.27kW less than that in the case of constant device. The average and the maximum

Table 3. Power consumption (PC) in variable and constant mass cases at the feed rate of 7 kg s^{-1}.

Working device	PC in variable mass (kW)		PC in constant mass (kW)		Difference between the variable mass and the constant mass (kW)	
	Maximum value	Average value	Maximum value	Average value	Maximum value	Average value
Tangential-flow drum	23.33	12.84	17.34	9.75	5.99	3.09
Auxiliary feed beater	15.82	6.78	16.31	8.43	-0.49	-1.65
Longitudinal-axis drum	66.17	52.77	87.24	64.94	-21.07	-12.17

Table 4. Power consumption (PC) in variable and constant mass cases at the feed rate of 6 kg s^{-1}.

Working device	PC in variable mass (kW)		PC in constant mass (kW)		Difference between the variable mass and the constant mass (kW)	
	Maximum value	Average value	Maximum value	Average value	Maximum value	Average value
Tangential-flow drum	20.59	10.52	16.31	7.79	4.28	2.73
Auxiliary feed beater	11.14	4.32	11.51	5.56	-0.37	-1.24
Longitudinal-axis drum	53.21	43.96	71.97	54.4	-18.76	-10.44

[DOR: 20.1001.1.16807073.2013.15.7.20.9]

Table 5. Power consumption (PC) in variable and constant mass cases at the feed rate of 5 kg s^{-1}.

Working device	PC in variable mass (kW)		PC in constant mass (kW)		Difference between the variable mass and the constant mass (kW)	
	Maximum value	Average value	Maximum value	Average value	Maximum value	Average value
Tangential-flow drum	17.36	8.67	13.72	6.51	3.64	2.16
Auxiliary feed beater	8.04	3.84	8.31	4.70	-0.27	-0.86
Longitudinal-axis drum	49.75	35.66	63.94	42.98	-14.19	-7.32

power consumption of the longitudinal-flow drum in variable mass were, respectively, 7.32 and 14.19kW less than that in the constant mass case. Based on these results, as the feed rate increased, the maximum and average power consumption of the tangential-flow drum and longitudinal-flow drum increased, due to the increased load of material flow.

CONCLUSIONS

The difference of the variable mass and constant mass threshing process was studied. The conclusions drawn from this study are summarized below:

1) The change in rates of material flow along the arc-length of concave in tangential-flow device and longitudinal-flow device are equal to the change in rates of material density with time. When the feed rate of the material of tangential-flow device was less than the feed rate of the material of longitudinal-flow threshing device and the feeding density of longitudinal-flow threshing device was more than the feeding density of tangential-flow device, the auxiliary feed device was in normal operation. Otherwise, the auxiliary feed device would be blocked up.

2) The experimental material flow rate was less than that of the theoretical material in the tangential-flow device and longitudinal-flow device at the feed rate of 5, 6, and 7 kg s^{-1}. In tangential-flow device, material flow rate of the tangential-flow device accounted for 81.47, 83.54, and 85.00% of the theoretical material feed rate at the feed rate of 5, 6, and 7 kg s^{-1}, respectively. In the longitudinal-flow device, the materials threshed and separated accounted for 40.80, 47.21, and 52.12% and the loss was 0.34, 0.55, and 0.79%, respectively. The material flow rates at the output parts were 3.37, 4.040 and 4.72 kg s^{-1}, respectively, which accounted for 67.32, 67.34 and 67.44 % of the theoretical material flow rate.

3) when the longitudinal-tangential flow device was at the feed rate of 5, 6, and 7 kg s^{-1} during the threshing process in variable and constant mass, the average and the maximum power consumptions of the tangential-flow drum in variable mass were respectively, 2.16, 2.73, and 3.09kW more than that in constant mass, while the maximum power consumption of the tangential-flow drum in variable mass was 3.64, 4.28 and 5.99kW more than that in constant mass, respectively. The average power consumption of the auxiliary feed beater in variable mass was 0.86, 1.24, and 1.65kW less than that in constant mass, while the maximum power consumption of the auxiliary feed beater in variable mass was 0.27, 0.37 and 0.49kW less than that in constant mass. The average power consumption of the longitudinal-flow drum in variable mass was 7.32, 10.44 and 12.17kW less than that in constant mass while the maximum power consumption of the longitudinal-flow drum in variable mass was 14.19, 18.76, and 21.07kW less than that in constant mass.

ACKNOWLEDGEMENTS

This research work was supported by Jiangsu Science and Technology Support Program Funded Projects (BE2011333), The Graduate Innovative Projects of Jiangsu Province (No.CXZZ11_0549), and A Project Funded by

[DOR: 20.1001.1.16807073.2013.15.7.20.9]

High-tech Key Laboratory of Agricultural Equipment and Intelligent technology of Jiangsu Province (No.BM2009703). The authors appreciate the helpful suggestions on the paper from the reviewers.

REFERENCES

1. Anil, J., Guruswamy, T. and Desai, S. R. 1998. Effect of Cylinder Speed and Feed Rate on the Performance of Thresher. *J. Agr. Sci.*, **4**: 1120–1123.
2. Burcev, P. 1963. Meshchersky's Equations in the General Theory of Relativity. *BAC*, **14**: 124–126.
3. Godwin, R. J., Wheeler, P. N., O'Dogherty, M. J., Watt, C. D. and Richards, T. 1999. Cumulative Mass Determination for Yield Maps of Non-grain Crops. *Comput. Electron. Agric.*, **23**: 85–101.
4. Harrison, H. P. 1991. Rotor Power and Losses of an Axial Flow Combine. *Trans. ASAE*, **34(1)**: 60–64.
5. Hennens, D., Baert, J., Baerdemaeker, J. D. and Ramon, H. 2003. Development of a Flow Model for Design of a Momentum Type Beet Mass Flow Sensor. *Biosys. Eng.*, **85(4)**: 425–436.
6. Huynh, V. M. and Powell, T. 1982. Threshing and Separating Process a Mathematical Model. *Trans. ASAE*, **20(1)**: 65–73.
7. Igathinathane, C., Womac, A. R., Sokhansanj, S. and Narayan, S. 2008. Knife Grid Size Reduction to Pre-process Packed Beds of High-and Low-moisture Switch Grass. *Biores. Technol.*, **99**: 2254–2264.
8. Kumara, A., Mohanb, D. and Patelb, R. 2002. Development of Grain Threshers Based on Ergonomic Design Criteria. *Appl. Ergon.*, **33**: 503–508.
9. Li, J., Yan, C. L. and Yang, F. F. 2006. Theoretical Model and Simulation of Threshing of Axial Unit with Axial Feeding. *J. Jiangsu University:NSE*, **27(4)**: 299–302.
10. Maertens, K. and Baerdemaeker, J. D. 2003. Flow Rate Based Prediction of Threshing Process in Combine Harvesters. *Appl. Eng. Agric.*, **19(4)**: 383–388.
11. Miu, P. I. and Kutzbach, H. D. 2007. Mathematical Model of Material Kinematics in an Axial Threshing Unit. *Comput. Electron. Agric.*, **58**: 93–99.
12. Miu, P. I. 2008. Modeling and Simulation of Grain Threshing and Separation in Axial Threshing Units, Part II: Application to tangential feeding. *Comput. Electron. Agric.*, **60(1)**: 105–109.
13. Mostofi, M. R. and Minaei, S. 2009. Mass Flow Rate Measurement System Performance on Potato Harvesters. *J. Agri. Sc. Tech.*, **11(1)**: 259–274.
14. Rahimi, M. Rabiei, B. Samizadeh, H. and Kafi Ghasemi, A. 2010. Combining Ability and Heterosis in Rice (*Oryza sativa* L.). *J. Agri. Sc. Tech.*, **12**: 223–231.
15. Rasouli, F., Sadighi, H. and Minaei, S. 2009. Factors Affecting Agricultural Mechanization: A Case Study on Sunflower Seed Farms in Iran. *J. Agri. Sc. Tech.*, **11**: 39–48.
16. Saeid, S., Mansoor, M., Lar, B. and Alisadi, J. 2006. A New Design for Grain Combine Thresher. *Int. J. Agri. Biol.*, **8(5)**: 680–683.
17. Sudajana, S., Salokhea, V. M. and Triratanasirichaib, K. 2002. Effect of Type of Drum, Drum Speed and Feed Rate on Sunflower Threshing. *Biosys. Eng.*, **83(4)**: 413–421.
18. Su, X. Y., Wu, J. Y., Zhang, H. J., Li, Z. Q., Sun, X. H. and Deng, Y. 2012. Assessment of Grain Security in China by Using the AHP and DST Methods. *J. Agri. Sc. Tech.*, **14**: 715–726.
19. Szymanek, M. 2008. Evaluation of Quantitative and Qualitative Losses of the Cutting Process for Sweet Corn Kernels. *Appl. Eng. in Agric.*, **24(5)**: 559–563.
20. Tang, Z., Li, Y. M. and Xu, L. Z. 2011. Effects of Different Threshing Components on Grain Threshing and Separating by Tangential-axial Test Device. *Trans. CSAE*, **27(3)**: 93–97.
21. Vejasit, A. and Salokhe, V. M. 2005. Studies on Machine-crop Parameters of an Axial Flow Thresher for Threshing Soybeans. *Agricultural Engineering International: The CIGR Journal of Scientific Research and Development*, Manuscript PM 04, 004.
22. Wacker, P. and Kutzbach, H. D. 2003. State of the Art of Combine Harvesters for grain Harvesting. *Harvest Technol.*, **58(4)**: 234–235.
23. Yang, F. F., and Yan, C. L. 2008. Movement Analysis of Cereal in Axial Flow Threshing Roller Space. *Trans. CSAE*, **39(11)**: 48–50.
24. Zhang, R. C. and Sang, Z. Z. 2000. Simulation Research on the Movement of Cereal in Axial Threshing Space. *Trans. CSAE*, **31(1):** 55–67.

[DOR: 20.1001.1.16807073.2013.15.7.20.9]

مطالعه خرمنکوبی برنج با دروگرکمباین دارای جریان مماسی-طولی در شرایط جرم متغییر

ت. ژانگ، ل. یاومینگ، و و. چنگهونگ

چکیده

مطالعات موجود در زمینه فرایند خرمنکوبی دروگرهای کمباین بر مبنای فرض ثابت بودن جرم هستند ولی این فرضیه در تضاد با پدیده جدا شدن دانه وکلش کوتاه در فرایند واقعی خرمنکوبی است. بنا براین، ویژگی های خرمنکوبی و جداسازی به گونه ای دقیق تشریح نمی شوند. با این هدف، در پژوهش حاضر دستگاه خرمنکوب و جدا ساز با جریان مماسی-طولی مجهز به وسیله جریان مماسی ، کوبنده تغذیه کننده کمکی ، و دستگاه جریان طولی مربوط به دروگر کمباین روی سکوی آزمون ساخته شد و با کار برد آن آزمونها و تحلیل های مورد نظر روی خرمنکوبی برنج با نرخ تغذیه ۵، ۶، و۷کیلو گرم بر ثانیه انجام شد.نتایج نشان داد که تغییرات نرخ جریان مواد در طول قوس ضد کوبنده در دستگاه جریان مماسی و دستگاه جریان طولی برابر با تغییرات نرخ چگالی مواد در گذر زمان است. در فرایند خرمنکوبی با جرم متغییر و جرم ثابت و در شرایط نرخ تغذیه ای ۵، ۶، و۷ کیلو گرم بر ثانیه در سکوی آزمون، مقدار جریان مواد از دستگاه جریان مماسی به ترتیب برابر بود با4.07 ، 5.01، **و** 5.95 $kg{\cdot}s^{-1}$. میانگین توان مصرفی استوانه جریان مماسی در فرایند خرمنکوبی با جرم متغییر به ترتیب ۲.۷۳،۲.۱۶، و۳.۰۹کیلو وات بیشتر از خرمنکوبی با جرم ثابت بود.نرخ جریان در خروجی دستگاه جریان -طولی به ترتیب برابر ۴.۰۴،۳.۳۴، و۴.۷۲ کیلو گرم بر ثانیه بود.از سوی دیگر، میانگین توان مصرف شده استوانه جریان- طولی در فرایند خرمنکوبی با جرم متغییر به ترتیب ۱۰.۴۴،۷.۳۲، و ۱۲.۱۷ کیلو وات کمتر از خرمنکوبی با جرم ثابت بود.این گونه نتایج مربوط به نرخ جریان مواد و مصرف توان میتواند مبنای طراحی دستگاه خرمنکوبی و جدا سازی مجهز به جریان طولی-مماسی قرار گیرد.

[DOR: 20.1001.1.16807073.2013.15.7.20.9]